UNIUNEA EUROPEANĂ

GUVERNUL ROMÂNIEI
MINISTERUL MUNCII, FAMILIEI
ŞI
PROTECŢIEI SOCIALE
AMPOSDRU

Fondul Social European
POSDRU 2007-2013

Instrumente Structurale
2007-2013

OIPOSDRU

UNIVERSITATEA BABEŞ-BOLYAI
CLUJ-NAPOCA

Investing in people!

Ph.D. scholarship, Project co-financed by the SECTORAL OPERATIONAL PROGRAM FOR HUMAN RESOURCES DEVELOPMENT 2007 - 2013
Priority Axis 1. "Education and training in support for growth and development of a knowledge based society"
Key area of intervention 1.5: Doctoral and post-doctoral programs in support of research.
Contract no.: POSDRU/88/1.5/S/60185 – "INNOVATIVE DOCTORAL STUDIES IN A KNOWLEDGE BASED SOCIETY"
Babeş-Bolyai University, Cluj-Napoca, Romania

BABEŞ-BOLYAI UNIVERSITY, CLUJ-NAPOCA, ROMANIA

FACULTY OF CHEMISTRY AND CHEMICAL ENGINEERING

THE RECOVERY AND THE PRACTICAL APPLICATIONS OF NICKEL FROM WASTE ELECTRICAL AND ELECTRONIC EQUIPMENTS

PhD Thesis abstract

Scientific supervisor	***PhD. Student***
Prof. Dr. Eng. Petru ILEA	**Eng. Bianca ROBOTIN**
	(b. IORDACHE)

CLUJ-NAPOCA

2012

TABLE OF CONTENTS

PART I.

LITERATURE OVERVIEW

1. GENERAL ASPECTS OF THE IMPORTANCE OF NICKEL 3

1.1. General aspects 3

1.2. Nickel toxicity 3

1.3. Sources of nickel pollution 4

1.4. Nickel's impact on plants, animals and humans 5

1.5. Economic aspects 6

  1.5.1. Nickel's price evolution in the last 10 years 6

1.6. Nickel applications 9

1.7. Nickel modern applications 9

2. NICKEL RECOVERY FROM WASTE ELECTRICAL AND ELECTRONIC EQUIPMENTS (WEEE) 10

2.1. EU WEEE Directives 10

2.2. WEEE Structure 11

2.3. WEEE Dismantling 13

2.4. Techniques for WEEE treatment 14

  2.4.1. Physical-chemical processes 15

    2.4.1.1. Precipitation 15

    2.4.1.2. Flotation 16

    2.4.1.3. Ultra-filtration 17

    2.4.1.4. Nano-filtration 18

    2.4.1.5. Reverse osmosis 18

    2.4.1.6. Ionic exchange 19

    2.4.1.7. Adsorption 20

  2.4.2. Electrochemical processes 20

    2.4.2.1. Electro-dialysis 20

2.4.2.2. Electro-coagulation 21
2.4.2.3. Electro-flotation 22
2.4.2.4. Electro-deionization 22
2.4.2.5. Electrodeposition 22
2.5. Nickel recovery from other sources 25
2.5.1. Nickel recovery from spent solutions 25
2.5.2. Nickel recovery from spent batteries 25
2.5.3. Nickel recovery from spent catalysts 26
2.5.4. Other sources 27

3. NICKEL ELECTRODEPOSITION FROM AQUEOUS SULPHATE AND CHLORIDE SOLUTIONS 28
3.1. Nickel electrodeposition mechanism 29
3.1.1. Nickel electrodeposition mechanism from sulphate solutions 29
3.1.2. Nickel electrodeposition mechanism from chloride solutions 30
3.1.3. Differences between the electrodeposition mechanisms 32
3.2. Parameters which influence the nickel electrodeposition 33
3.2.1. Electrolyte composition 33
3.2.2. The effect of pH and temperature 33
3.2.3. Additives used in electrolyte solutions for nickel electrodeposition 34
3.2.4. Substrates used for nickel electrodeposition 35
3.3. Interfering metals with nickel electrodeposition 36

4. THE ELECTRODEPOSITION OF Ni-Fe ALLOYS 39
4.1. Applications of Ni-Fe alloys 40
4.2. Electrolytes composition used in the electrodeposition of Ni-Fe alloys and types of Ni-Fe alloys 40
4.3. Parameters which influence the electrodeposition of Ni-Fe alloys 42
4.3.1. Electrolyte composition 43
4.3.2. Current density 43

4.3.3. Electrolyte pH 44
4.3.4. Additives 44
4.4. Ni-Fe alloys electrodeposition mechanism 45
CONCLUSIONS FOR THE LITERATURE OVERVIEW 47

PART II. PERSONAL CONTRIBUTIONS

5. INVESTIGATIVE TECHNIQUES FOR THE STUDIED SYSTEMS 48
5.1. Electrochemical methods 48
5.1.1. Linear and cyclic voltammetry 49
5.1.2. Hydrodynamic voltammetry on rotating disc electrode 50
5.1.3. Square wave voltammetry 51
5.1.4. Chronoamperometry (Potential step - PS) 52
5.2. Structural analyses methods (non-electrochemical) 54
5.2.1. X Ray Diffraction (XRD) 54
5.2.2. Scanning Electron Microscopy (SEM) 55
5.2.3. Flame Atomic Absorption Spectroscopy (FAAS) 56
5.2.4. X-Ray Fluorescence Spectrometry (XRFS) 57
5.2.5. Energy-Dispersive X-ray Spectroscopy (EDX) 58

6. PRELIMINARY STUDIES ON WASTE ELECTRIC AND ELECTRONIC EQUIPMENTS (WEEE) COMPOSITION AND SOLUBILIZATION TESTS 59
6.1. Why recycle WEEE? 59
6.2. Wastes types used for nickel recovery 61
6.3. WEEE situation in Romania 62
6.4. Preliminary processing methods of cathode ray tubes (CRT) wastes 63
6.5. The chemical composition of CRT wastes which contain nickel 64
6.6. The chemical and electrochemical solubilisation of the cathode ray tubes wastes which contain nickel 66

6.6.1. The chemical solubilisation of CRT wastes 67
  6.6.1.1. The chemical solubilisation of the electron gun (EG) 67
    6.6.1.1.1. The chemical solubilisation in H_2SO_4 67
    6.6.1.1.2. The chemical solubilisation in HCl 69
    6.6.1.1.3. The chemical solubilisation using oxidizing agents 70
6.6.2. The electrochemical solubilisation CRT wastes 71
  6.6.2.1. The experimental setup 71
  6.6.2.2. The solubilisation of magnetic components (EGM) 72
    6.6.2.2.1. Preliminary solubilisation tests 72
    6.6.2.2.2. The EGM wastes solubilisation in stages 72
  6.6.2.3. The electrochemical solubilisation of the shadow mask (SM) 75
    6.6.2.3.1. Preliminary solubilisation tests 76
    6.6.2.3.2. The SM wastes solubilisation in stages 77
6.7. Partial conclusions 81

7. IRON SEPARATION FROM NICKEL CONTAINING CONCENTRATED SOLUTIONS 82
7.1. The electrochemical oxidation of Fe (II) to Fe (III) 82
  7.1.1. The experimental conditions 82
  7.1.2. The experimental setup 84
  7.1.3. The experimental results 84
  7.1.4. Partial conclusions 86
7.2. The chemical separation of iron from solutions which contain nickel 86
  7.2.1. The experimental conditions 87
  7.2.2. Iron (III) separation from nickel containing solutions resulted from Fe (II) oxidation 88
  7.2.3. Iron (III) separation from synthetic solutions with similar composition as the solutions resulted from waste solubilisation 90
    7.2.3.1. The operations scheme 91
    7.2.3.2. The pH evolution in time 94

7.2.3.3. The amount of removed iron 97

7.3. Partial conclusions 99

8. NICKEL ELECTRODEPOSITION FROM DILUTE SULPHATE SOLUTIONS 100

8.1. Preliminary studies of linear voltammetry (LSV) 100

8.2. The nickel electrodeposition from dilute sulphate solutions 105

8.2.1. The experimental conditions 105

8.2.2. The experimental results 107

8.2.3. SEM images 111

8.2.4. Partial conclusions 113

8.3. The influence of Co and Mn on the nickel electrodeposition process 114

8.3.1. Preliminary studies of cyclic voltammetry 114

8.3.2. The experimental conditions for Ni electrodeposition from solutions containing Co and Mn 122

8.3.3. The experimental results 123

8.3.4. SEM images 131

8.3.5. EDX analysis 132

8.3.6. Partial conclusions 138

9. Ni-Fe ALLOYS ELECTRODEPOSITION FROM DILUTE SULPHATE SOLUTIONS 139

9.1. Preliminary studies of cyclic voltammetry (CV) 139

9.2. Ni-Fe alloys electrodeposition 142

9.2.1. The initial composition of the electrolyte 143

9.2.2. The experimental results 144

9.2.3. The determination of Ni-Fe alloys type co-deposition 150

9.2.4. SEM images 151

9.3. Partial conclusions 153

10. THE NUCLEATION MECHANISM FOR Ni, Fe AND Ni-Fe ALLOYS 155
10.1. Preliminary studies of cyclic voltammetry (VOC) 155
10.2. Chronoamperometric studies (potential step) 156
10.3. The determination of nucleation type 162
10.4. Partial conclusions 165

11. THE PROPOSED TEHNOLOGICAL FLOW DESCRIPTION 166

12. THE NICKEL RECOVERY FROM COMPUTER PRINTED CIRCUIT BOARDS (PCBs) 170
12.1. The chemical composition of PCBs 170
12.2. PCBs dismantling 170
12.3. The characterization of the electrolyte solution 174
12.4. The electrodeposition of Cu, Sn and Pb 177
12.5. The cementation of Ni with Zn 180
12.6. The proposed technological flow 182
12.7. Partial conclusions 184

GENERAL CONCLUSIONS 185
REFERENCES 189
FIGURES LIST 208
TABLES LIST 213
PUBLICATIONS AND CONFERENCES 216

KEYWORDS: nickel recovery, waste electrical and electronic equipments (WEEE), cathode ray tubes, computer printed circuit boards (PCBs), nickel electroextraction, Ni-Fe alloys and iron separation.

ABBREVIATIONS

AEM – anionic exchange membrane
BDL – below detected limit
CE – current efficiency
CRT – cathode ray tubes
E_B – cell voltage
EG – electron gun
EGM – electron gun magnetic components
EGN - electron gun non-magnetic components
IN – instantaneous nucleation
ND – not detected
PN – progressive nucleation
PCBs – printed circuit boards
SM – shadow mask
WEEE – waste electrical and electronic equipments
W_s – specific energy consumption

PERSPECTIVES AND AIMS OF THESIS

The current thesis is focussed on studying the recovery of nickel from waste electrical and electronic equipment (WEEE), and particularly from spent cathode ray tubes (CRTs) and computer printed circuit boards (PCBs).

PART I. LITERATURE OVERVIEW

The technological development over the past decades had the effect of a continuous increase in the use of heavy metals, with negative consequences for the environment. Nickel is one of the metals heavily used in modern technology. The accelerated consumption of nickel and nickel-containing products in various industrial stages resulted in the release of nickel into the environment [Widmer_2005, Robinson_2009, Babu_2007, Herat_2008, Nnorom_2010].

Electrical and electronic equipment (EEE) are developed, applied and used worldwide. Rapid changes in equipment features and capabilities, combined with a price decrease and an increased use of the Internet, are just a few factors that contributed to the accumulation of waste electrical and electronic equipment (WEEE). Following this massive development, the increasing amount of WEEE has become a significant problem all over the world. Given the harmful effects of WEEE on one hand, and the valuable materials that could be recovered and reused on the other hand, more and more countries have become concerned with WEEE management and with the development of efficient technologies for WEEE recycling [He_2006, Andreola_2005, Ongondo_2011, Bigum_2010, Lee_2002, Menad_1999].

Given the elevated nickel market price, the recycling of various wastes represents an attractive alternative for obtaining pure metallic nickel which could be reused in various fields [Robotin SS_2012].

Over the past years, various techniques have been developed for the treatment of heavy metal containing waste, all aiming to reduce the amount of waste generated and to improve the quality of their recycling.

The techniques used in treating heavy metals containing waste are divided into:

- Physicochemical methods: precipitation, flotation, ultrafiltration, nanofiltration, reverse osmosis, ion exchange, and adsorption.
- Electrochemical methods: electrodialysis, electrocoagulation, electroflotation, electrodeionization, and electrodeposition.

PART II PERSONAL CONTRIBUTIONS

5. INVESTIGATIVE TECHNIQUES FOR THE STUDIED SYSTEMS

The investigative techniques used in the current thesis can be divided into electrochemical methods and structural methods (non-electrochemical).

The electrochemical methods were cyclic voltammetry, linear sweep voltammetry, hydrodynamic voltammetry at a rotating disk electrode, square wave voltammetry, chronoamperomety (potential step) [Vârvara_2008, Turdean_2012, Bard_2001].

The structural methods complement the information given by electrochemical methods. From this category we can mention: X-ray diffraction, scanning electron microscopy, flame atomic absorption spectroscopy, X-ray fluorescence spectroscopy, X-ray spectroscopy, and energy-dispersive X-ray spectroscopy [Borodi_2012, Tudoran_2012, Broekaert_2002, Havrilla_1997, Sneddon_1997].

6. PRELIMINARY STUDIES ON WASTE ELECTRIC AND ELECTRONIC EQUIPMENTS (WEEE) COMPOSITION AND SOLUBILISATION TESTS

Cathode ray tubes (CRTs) are used in television displays and computer monitors. In Figure 1 an electron gun (EG) and a shadow mask (SM) are depicted, after being separated from a spent CRT. The two metallic components shown in Figure 1 contain a significant amount of nickel. The EG metal components were separated and used together with the fragments from the SM in studies aiming at Ni recovery [Robotin JE_2011].

For a quantitative analysis the EG metallic fractions were separated into magnetic components (EGM) and non-magnetic components (EGN). Table 1 presents a concentration range for the metals in EG and SM. In the EG case the tests were conducted on all three categories, namely unseparated EG, EGM and EGN.

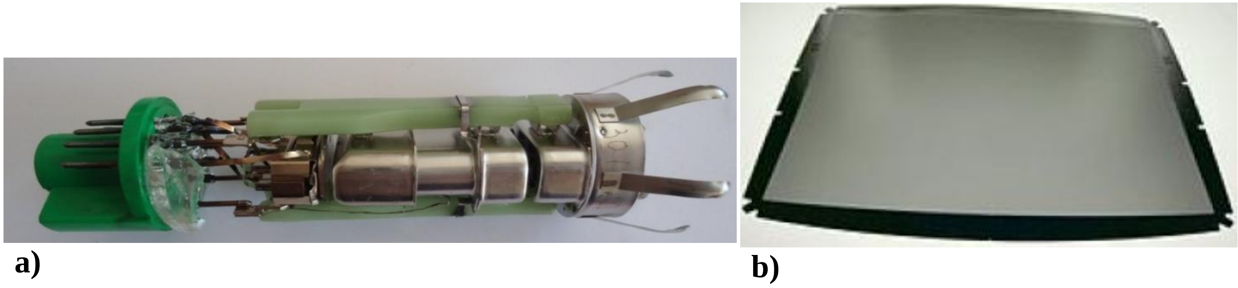

Figure 1 Images for the electron gun (EG) (a) and the shadow mask (SM) (b)

Table 1 The elemental composition of the EG and SM metallic components from a CRT [Robotin JE_2011]

CRT waste	**Ni**	**Fe**	**Cr**	**Mn**	**Co**
	[%]				
EG	25-30	50-60	10-11	1.0-1.5	1-2
EGM	40-45	50-55	ND*	0.3-0.35	3-3.5
EGN	10-15	60-70	17-19	1.0-1.5	ND*
SM	36-40	60-64	ND*	ND*	ND*

*Not detected

EG, EGM and EGN were subjected to both chemical and electrochemical leaching in various conditions. Table 2 summarizes the advantages and disadvantages of chemical and electrochemical leaching. The best results in our case were obtained when using a 2M H_2SO_4 solution, both for chemical and for electrochemical leaching. However, given the disadvantages of chemical leaching, the electrochemical dissolution proved to be the best choice in our case **[**Robotin Romphyschem_2010, Robotin JE_2011, Robotin_2011].

Table 2 The advantages and the disadvantages of the chemical and electrochemical solubilisation as a function of the waste type and the solubilisation medium

Waste type	**Chemical solubilisation**			**Waste type**	**Electrochemical solubilisation**		
	Solubilisation medium	**Advantages**	**Disadvantages**		**Solubilisation medium**	**Advantages**	**Disadvantages**
EG, EGM, EGN	18 M H_2SO_4	-	Ineffective – surface passivation [Abd_2003]	EGM, SM	1 M HCl	-	The precipitation of nickel hydroxide
	2 M H_2SO_4	Efficient – 44.3 % dissolved	Long solubilisation time (days) Higher amounts of acid		0.1 M NaCl pH = 1	-	The precipitation of nickel hydroxide
	1, 2, 4, 6 and 12 M HCl	Total solubilisation for concentration higher than 6 M	Long solubilisation time (days) Higher amounts of acid High toxicity		**2 M H_2SO_4**	Short solubilisation time (hours) Solubilisation in 4 steps with the metals concentration in the solution	-
	$FeCl_3$ in HCl	High solubilisation degree (higher than 70 %)	Long solubilisation time (days) Strong corrosion medium				

7. IRON SEPARATION FROM NICKEL CONTAINING CONCENTRATED SOLUTIONS

As already shown, the solutions resulted from the dissolution of solid waste (EG and SM) contain, besides Ni, significant quantities of Fe. Fe separation in this case is an important step because Ni electrodeposition is hampered by the presence of Fe in solution. Fe (present in the solution resulting from waste leaching) was subjected to an electrochemical treatment (oxidation) in order to convert it to Fe (III). In this situation, an efficient separation of Fe (III) from Ni containing solutions can be achieved by precipitation. It is worth mentioning that, according to the literature, Ni (II) and Fe (II) ions precipitation occurs at pH value higher than 6 [Sist_2003, Wei_2005, Bhattacharjee_2004]. Contrarily, Fe (III) ions precipitate at pH 4 [Wei_2005]. As a consequence, this pH difference makes possible the Fe separation from Ni containing solutions, if all Fe is in the +3 oxidation state [Wang_2011, Wang_2012, Chang_2010, Dousma_1976].

The electrochemical oxidation of Fe (II) was carried out in a two-compartment electrochemical reactor equipped with an anion exchange membrane (AEM). In the cathode compartment, the electrodeposition of Ni from concentrated sulphate solutions takes place while the oxidation of Fe (II) to Fe (III) occurs in the anode compartment.

The material balance for the electrochemical oxidation of Fe (II) to Fe (III) process is given in Table 3.

Table 3 The material balance for the electrochemical oxidation of Fe (II) to Fe (III)

Materials in [g]				**Materials out [g]**			
Anolyte	**Fe^{2+}**		1.0	**Anolyte**	**Fe^{3+}**		1.0
	Ni^{2+}		1.0		**Ni^{2+}**		1.0
Catolyte	**Ni^{2+} - solution**		5.6	**Catolyte**	**Ni^{2+} - solution**		5.0
					Ni^{2+} - deposit		0.6
TOTAL	**Anolyte**	**Fe^{2+}**	**1.0**	**TOTAL**	**Anolyte**	**Fe^{3+}**	**1.0**
		Ni^{2+}	**1.0**			**Ni^{2+}**	**1.0**
	Catolyte	**Ni^{2+}**	**5.6**		**Catolyte**	**Ni^{2+}**	**5.6**

The current efficiency and specific energy consumption were calculated for each compartment. The mean values obtained for the two compartments of the electrochemical reactor are given in Table 4.

Table 4 The current efficiency and specific energy consumption for each compartment of the reactor used for electrochemical oxidation of Fe (II) to Fe (III)

Compartment	**Current efficiency, CE [%]**	**Cell voltage, E_B [V]**	**Specific energy consumption, W_s [kWh/kg]**
Anode	100	3.45	3.45
Cathode	55		5.65

Table 5 contains the results of the separation experiments of Fe(III) from the Ni containing solutions with respect to the Fe amount removed from the filtrate and the amount of Ni lost in the precipitate, depending on temperature and neutralizing agent concentration [Robotin_2012b].

Table 5 Experimental data for the iron amount removed from the solution and the nickel loss in the precipitate [Robotin_2012b]

Na_2CO_3 [%]	**T [°C]**	**Ni loss [%]**	**Fe precipitate [%]**
5	25	5.6	99.8
10		11.3	99.5
5	50	12.5	99.9
10		19.2	99.8
5	**80**	**0.4**	**99.9**
10		**0.9**	**99.8**

The minimum Ni loss in the precipitate was obtained when working at 80 °C; the percentage of Ni lost by precipitation was below 1% for both concentrations of neutralizing agent. On the other hand, the Fe amount separated by precipitation is higher than 99.5% for all three studied temperatures and for both concentrations of the neutralizing agent, respectively [Robotin_2012b].

8. NICKEL ELECTRODEPOSITION FROM DILUTE SULPHATE SOLUTIONS

Ni electrodeposition is the final process stage in which metallic Ni is obtained by depositing it on the cathode. The composition of the electrolyte solution for the Ni electrodeposition tests was similar to the composition of the solution resulting from the dissolution of waste CRT components [Robotin JE_2011, Coman RICCCE_2011].

The aim of the Ni electrodeposition tests was the finding of optimal parameters for Ni recovery from dilute solutions. The influence of pH and initial concentration of Ni^{2+} were evaluated. The experiments were performed in galvanostatic mode.

The current efficiency was evaluated for each experiment, in order to establish the efficiency of Ni electrodeposition from dilute sulphate solutions and the results are presented (Figure 2) as a function of initial pH and different Ni concentrations. The maximum current efficiency values (around 76%) when working at low pH (pH 2), were obtained at high concentrations of Ni^{2+}. The current efficiency varies depending on the Ni concentration in a range between 52 and 76%. Current efficiency increases with increasing pH, reaching a value of 95% for pH 3 and 4 and high concentrations of Ni^{2+} [Robotin_2012a].

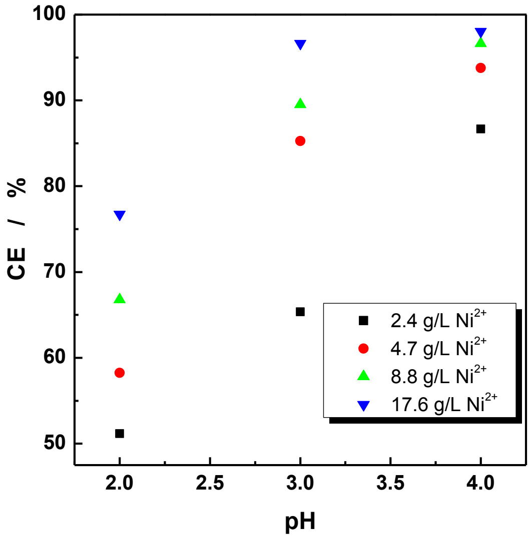

Figure 2 The pH influence on the current efficiency for different nickel initial concentration in the electrolyte

The specific energy consumption was evaluated for all Ni electrodeposition tests and the results are given in Table 6.

Table 6 The specific energy consumption function of the nickel initial concentration, for different pH values. Comparison with some literature data [Robotin_2012a]

Personal results				**Literature data**			**References**
[Ni^{2+}] g/L	**pH**			**[Ni^{2+}] g/L**	**pH**		
	2	**3**	**4**		**1.5**	**5**	
	kWh / kg Ni				**kWh / kg Ni**		
2.4	7.1	7.1	5.4	0.5	39.84*	-	*[Kaminari_2007]
4.7	5.5	4.2	3.9	0.75	32.80*	-	
8.8	4.3	3.4	3.0	10	-	26.80**	**[Agrawal_2007]
17.6	3.3	2.7	2.6	20	-	19.05**	

As can be seen from Table 6, the specific energy consumption is lowered when the initial concentration of Ni^{2+} and pH increase. As expected, the electrodeposition process is favoured by high concentrations of Ni^{2+} and elevated pH, when the hydrogen evolution reaction (HER) has less impact on the entire process [Robotin_2012a].

SEM images were taken for all obtained deposits, and the resulted pictures are shown below in Figure 3.

The images shown in Figure 3 reveal that at low concentrations of Ni^{2+} (2.4 and 4.7 g/L) the obtained deposits are uniform, their grains having about the same size for all studied pH values. At higher concentrations of Ni^{2+} (8.8 g L) at pH 2 and 3, the grain size increases, while at pH 4, the obtained deposits are not uniform and present surface cracks. The deposits obtained at the highest tested Ni concentration (17.6 g/L) have surface cracks for all studied pH values. This behaviour can be explained by the fact that under these conditions the charge transfer step is fast making the formation of the new solid phase the rate-limiting step, and, as a consequence, the deposit doesn't develop/grow uniformly [Robotin_2012a].

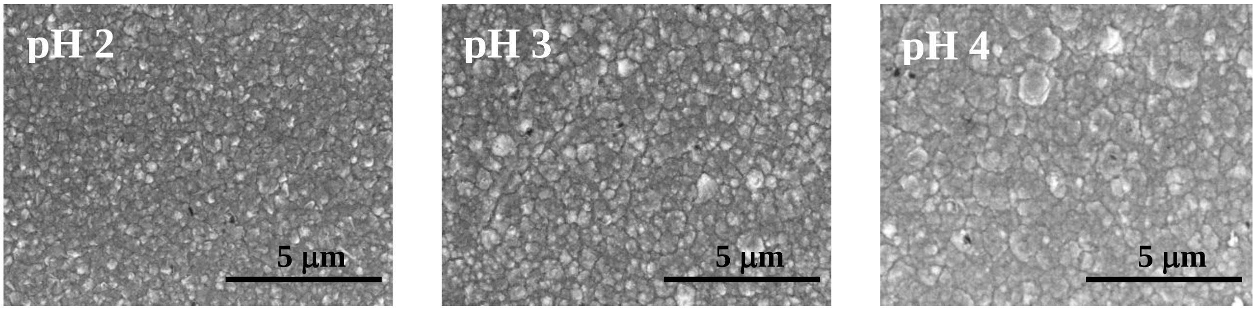

2.4 g/L Ni^{2+}

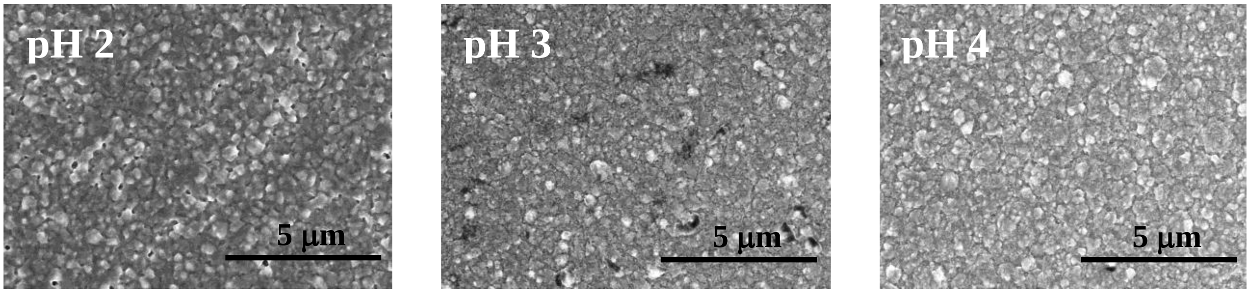

4.7 g/L Ni^{2+}

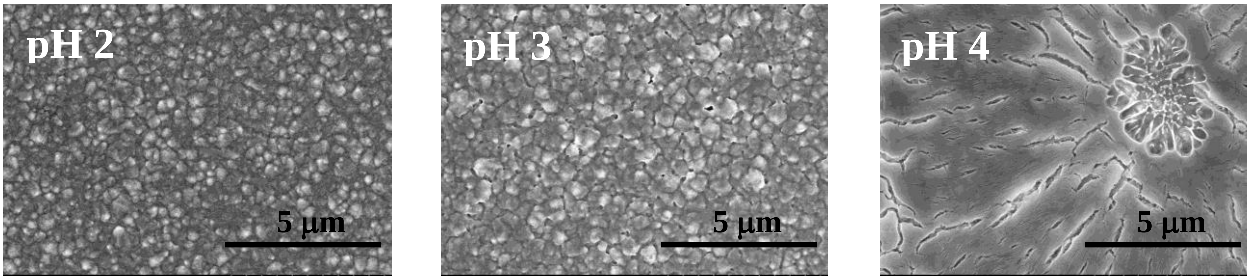

8.8 g/L Ni^{2+}

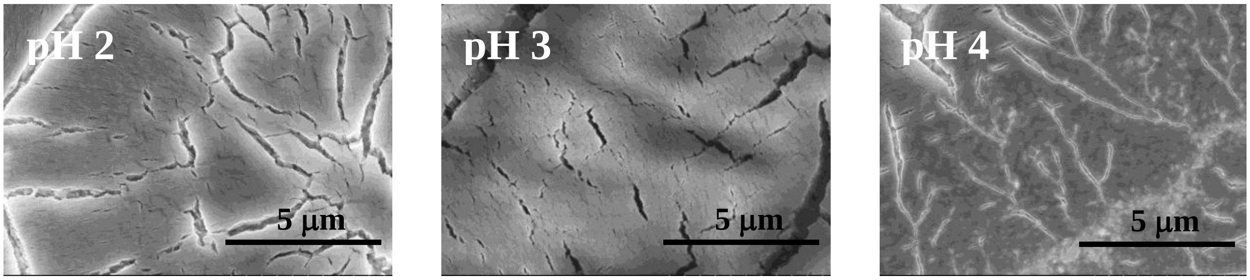

17.6 g/L Ni^{2+}

Figure 3 SEM images for the deposits obtained by nickel electrodeposition from sulphate solutions with contain 2.4, 4.7, 8.8 and 17.6 g/L Ni^{2+} at 2 A/dm^2, pH 2, 3 and 4, T = 60 °C

EG waste elemental analysis revealed the existence of two predominant metals: Ni and Fe and the presence of low concentrations of other metals (impurities): Co and Mn in the EGM components. The influence of Co and Mn impurities on the electrodeposition of Ni from sulphate solutions was evaluated. The electrodeposition tests were performed on synthetic solutions with Co and Mn concentrations similar to the real solution resulting from the EGM waste leaching.

The current efficiency and specific energy consumption for the electrodeposition of Ni from solutions containing Co and Mn at different pH values were evaluated. The obtained values are summarized in Table 7. In all presented cases, the current efficiency is higher than 60%, except for the result obtained for the electrodeposition of Ni in the presence of Mn at pH 4, when the current efficiency was as low as 37%. Concerning the specific energy consumption, it ranges between 3.8 and 6.7 kWh/kg of Ni deposit.

Table 7 The current efficiency and the specific energy consumption for nickel electrodeposition from solutions which contain Co and Mn

Electrolyte	**pH**	**Current efficiency, CE [%]**	**Voltage, E_B [V]**	**Specific energy consumption, W_s [kWh/kg deposit]**
Ni - Co	**2**	74	3.65	4.5
	3	71	3.78	4.9
	4	64	3.85	5.5
Ni - Mn	**2**	63	3.83	5.6
	3	67	4.93	6.7
	4	37	5.55	13.7
Ni – Co - Mn	**2**	61	3.63	5.4
	3	92	3.83	3.8
	4	81	3.95	4.5

9. Ni-Fe ALLOYS ELECTRODEPOSITION FROM DILUTE SULPHATE SOLUTIONS

EG waste leaching resulted in solutions containing large amounts of Ni and Fe. In order to recycle these types of waste, the electrodeposition of Ni-Fe alloys was tested. The tests were performed on synthetic solutions with a composition similar to real solutions obtained by dissolving the waste. The influence of current density and Ni/Fe ratio in the initial electrolyte solution were evaluated in order to determine the type of alloy which is obtained under these conditions [Robotin_2012a, Robotin_RSE_SEE_2012].

In Figure 4 the current efficiency dependence on the current density it is shown for the electrodeposition of Ni-Fe alloys from sulphate solutions. From Figure 4 it is observed that the current efficiency is higher than 65% for experiments performed at current densities higher than 2 A/dm^2 [Robotin_2012a]. Moreover, it can be seen that with decreasing Fe concentration in the electrolyte solution, the current efficiency for the electrodeposition process increases. Gangasingh *et al.* obtained an average current efficiency around 85% when they worked under potentiostatic electrodeposition of Ni-Fe alloys, in the absence or in the presence of boric acid, respectively [Gangasing_1991].

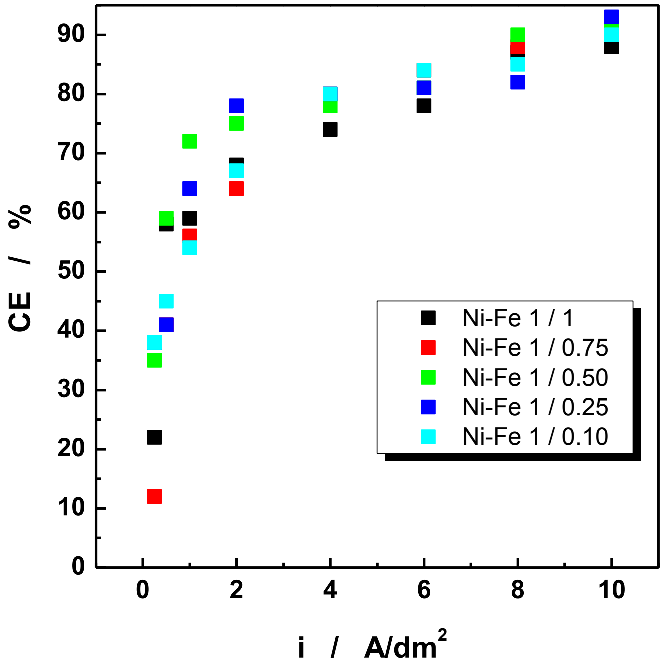

Figure 4 The current efficiency dependence on the current density in the Ni-Fe alloys electrodeposition process. Ni-Fe ratio in the initial electrolyte solution is shown in the figure. Experimental conditions: T = 60 °C, pH = 2

Figure 5 shows the current density influence on the content of Fe a), or Ni b) in the deposits obtained by galvanostatic electrodeposition from sulphate solutions for different ratios of Ni/Fe in the initial electrolyte solution. From the two representations it can be seen that there is no linear correlation of the amount of Fe or Ni with the current density. When the current density increases, it can be noticed that the deposition of Ni-Fe alloys is controlled by diffusion. The maximum value recorded at around 2 A/dm^2 indicates that the diffusion layer has less Fe. Above this value of current density the deposition process is controlled by diffusion. It can be also noted that at low current density (up to 2 A/dm^2), the Fe content in the deposit increases reaching a maximum, and at higher current densities the Fe content in deposit decreases [Robotin_2012a]. This tendency was observed in all the Ni-Fe reports studied and at different Ni and Fe concentrations. If the concentration of metal ions in the electrolyte increases, the Fe content in the deposit increases as well. Furthermore, the Fe content in the deposit decreases with increasing of the current density. These results are agreement with the literature data [Brenner_1963].

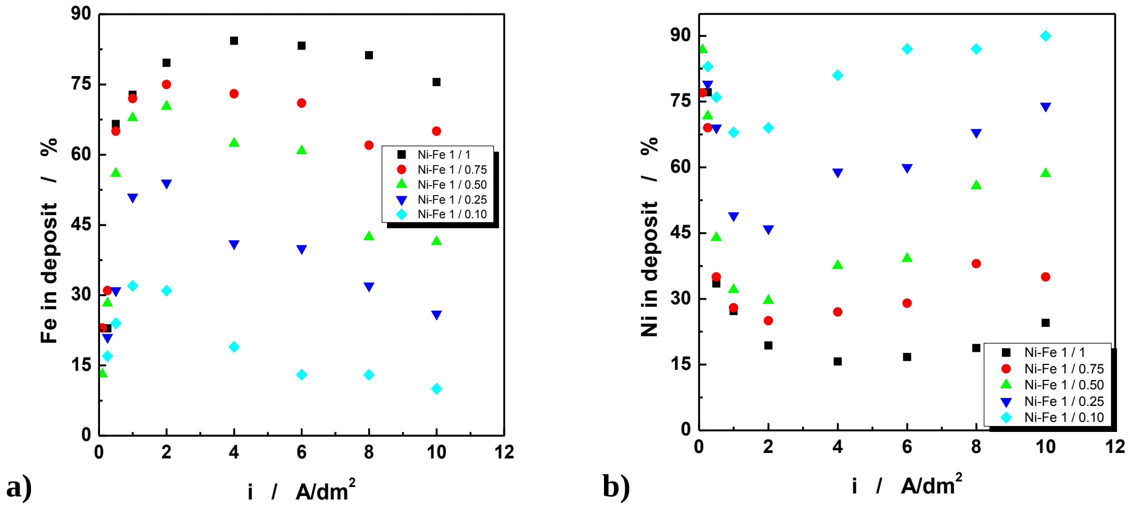

Figure 5 The current efficiency influence on the content of Fe a) and Ni b) in the Ni-Fe deposits obtained by electrodeposition from sulphate solutions, for different Ni-Fe ratio in the initial electrolyte solutions. Experimental conditions: see Figure 4

In most experimental conditions, the electrodeposition process of Ni-Fe alloys is classified as an "anomalous" co-deposition. This means that the less noble metal, in our case Fe, is deposited preferentially before Ni, which is more noble metal [Brenner_1963]. This behaviour is represented by the position of the data points above the reference concentration line AB. This type of co-deposition occurs at higher than 0.5 A/dm^2 values of current density. At low current densities (0.25 A/dm^2) the co-deposition process becomes "normal" as can be seen from Figure 6

[Robotin_2012a, Robotin ISE_2012]. Instead, at this value of current density (0.25 A/dm^2), the current efficiency is quite low (see Figure 4).

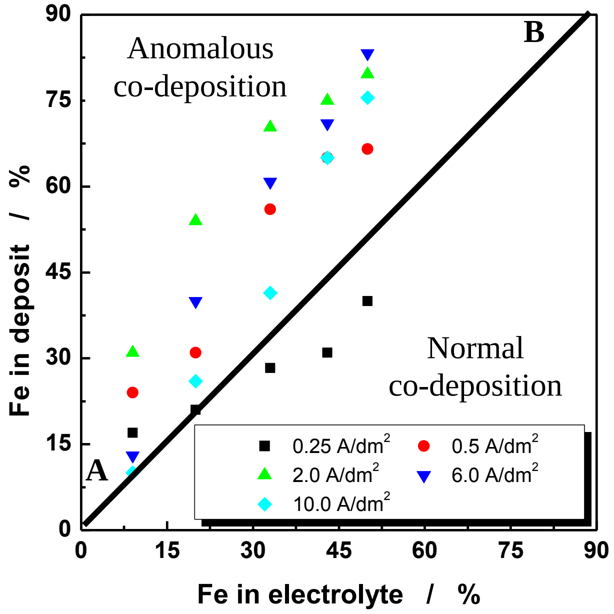

Figure 6 The interdependence of Fe content in the deposit on the iron content in the initial electrolyte solution. Experimental conditions: see Figure 4

The surface morphology of Ni-Fe alloy deposits was evaluated by SEM analysis [Robotin_2012a]. The images allowed highlighting the cracks on the surface of the obtained deposits. After analysing the literature, we can say that fissures/cracks appearing on the surface of Ni-Fe deposit are caused by the presence of Fe, because it generates severe tensions inside the deposit [Brenner_1963].

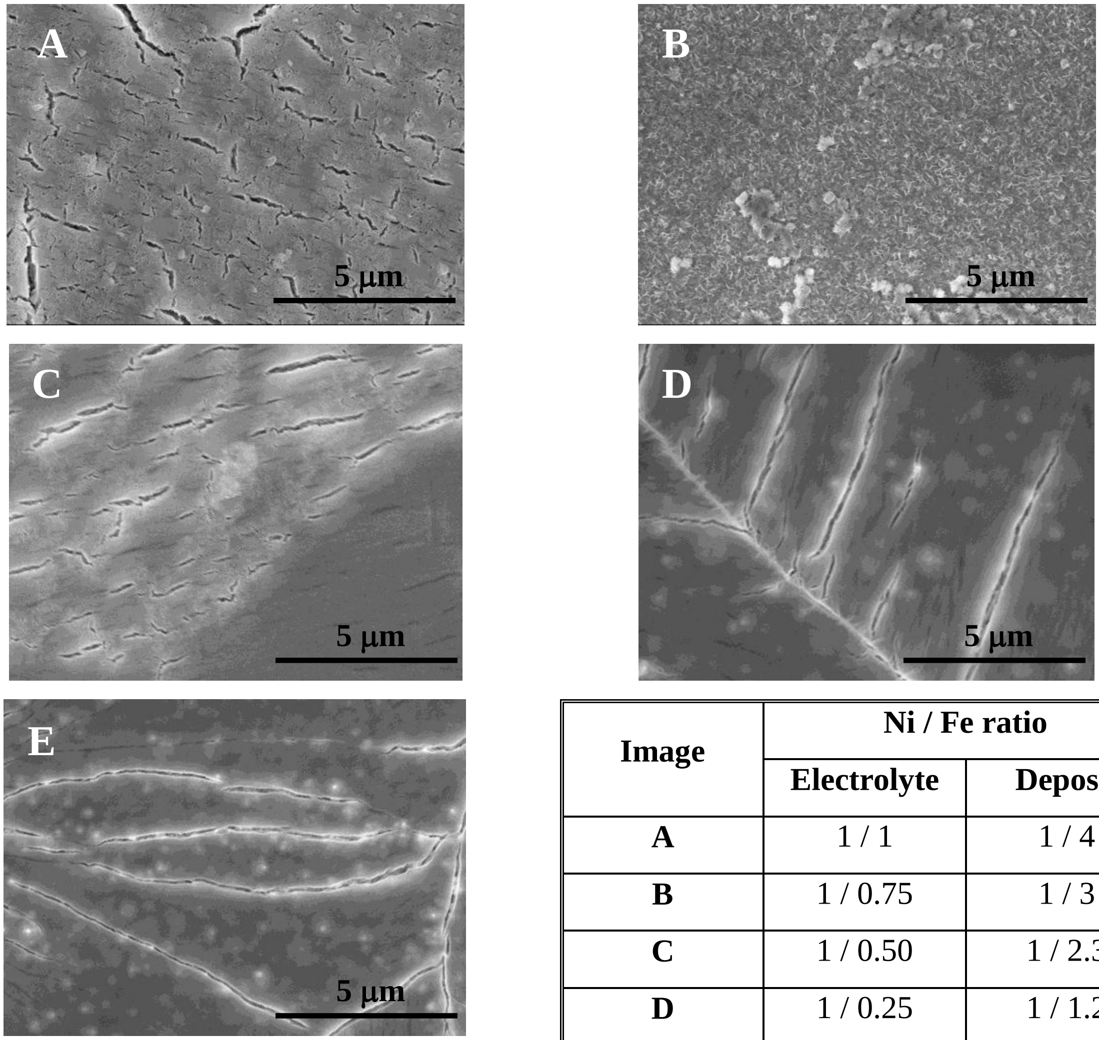

Image	Ni / Fe ratio	
	Electrolyte	**Deposit**
A	1 / 1	1 / 4
B	1 / 0.75	1 / 3
C	1 / 0.50	1 / 2.3
D	1 / 0.25	1 / 1.2
E	1 / 0.10	2.3 / 1

Figure 7 SEM images for Ni-Fe alloys deposited from sulphate solutions (see table inset), in galvanostatic conditions (i_c = 2 A/dm^2). Experimental conditions: see Figure 4

10. THE NUCLEATION MECHANISM FOR Ni, Fe AND Ni-Fe ALLOYS

Typical voltammograms for Ni, Fe and Ni-Fe, recorded at a Cu electrode at pH 3 are shown in Figure 8 [Robotin_2012a]. The differences between the three cases can be seen by examining in detail the cathodic curve (graph insert). The reduction peak corresponding to Ni is located at about -1.05 V *vs.* RE, while the Fe reduction process occurs at -1.15 V. As expected, the peak corresponding to the reduction of a Ni-Fe alloy is situated between the peaks corresponding to Ni and Fe, at about -1.11 V *vs.* RE. In the anodic region, where the dissolution takes place, the differences between the three cases are clearer. The Ni oxidation peak, situated at

-0.2 V, is very small due to the passivation of Ni in the sulphate medium. The peak corresponding to Fe oxidation is higher and is around the potential of -0.54 V. The voltammograms recorded for Ni-Fe complex shows an oxidation peak at -0.28 V. In the case of Fe and Ni-Fe, the anode curves intersect the cathode curves at low potentials, suggesting that the deposit grows better on the newly formed layer compared to the initial Cu substrate [Pletcher_1991].

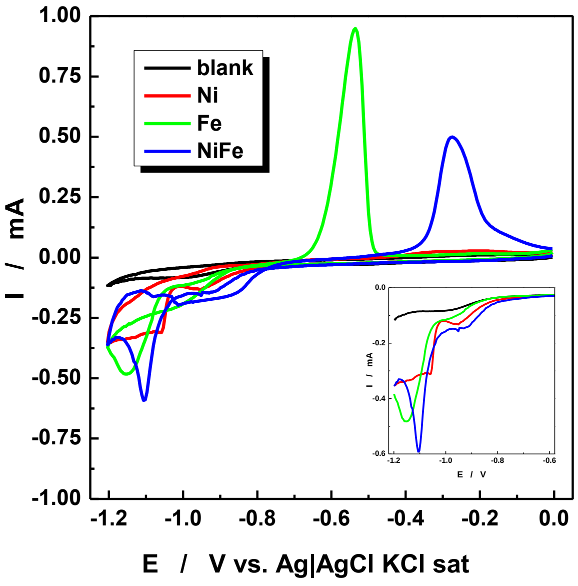

Figure 8 Cyclic voltammograms for 0.04 M Ni, Fe and Ni-Fe in 0.5 M Na_2SO_4, recorded on Cu electrode, at pH 3. Scanning rate 5 mV/s. The inset graph shows a detail of the cathodic section where the metallic ions reduction occurs.

The chronoamperometry tests aimed at determining the nucleation mechanism for the electrodeposition of Ni, Fe and Ni-Fe alloy from sulphate solutions and to find an explanation for the cracks occurrence on the surface of Ni and Ni-Fe deposits, revealed by the SEM images [Robotin_2012a].

If the case of the curves shown in Figure 9, the recorded currents recorded for the blank solution were extracted from the corresponding metal ions currents. In all three cases, a single peak appears which is larger for Ni-Fe. The maximal currents (I_m) recorded are higher for Fe and Ni-Fe compared to Ni. The time values corresponding to the maximum current (I_m) were denoted by t_m. Since the deposition of the two metals is controlled by diffusion, we chose a simple model from the literature to correlate the experimental data obtained [Scharifker_1983, Su_2009].

According to the model, the equations that describe the nucleation type are:

$$\left(\frac{I}{I_m}\right)^2 = \frac{1.9542}{t/t_m}\left\{1 - exp\left[-1.2564\left(\frac{t}{t_m}\right)\right]\right\}^2 \qquad (1) \quad \text{for instantaneous nucleation (IN), and}$$

$$\left(\frac{I}{I_m}\right)^2 = \frac{1.2254}{t/t_m}\left\{1 - exp\left[-2.3367\left(\frac{t}{t_m}\right)^2\right]\right\}^2 \qquad (2) \quad \text{for progressive nucleation (PN).}$$

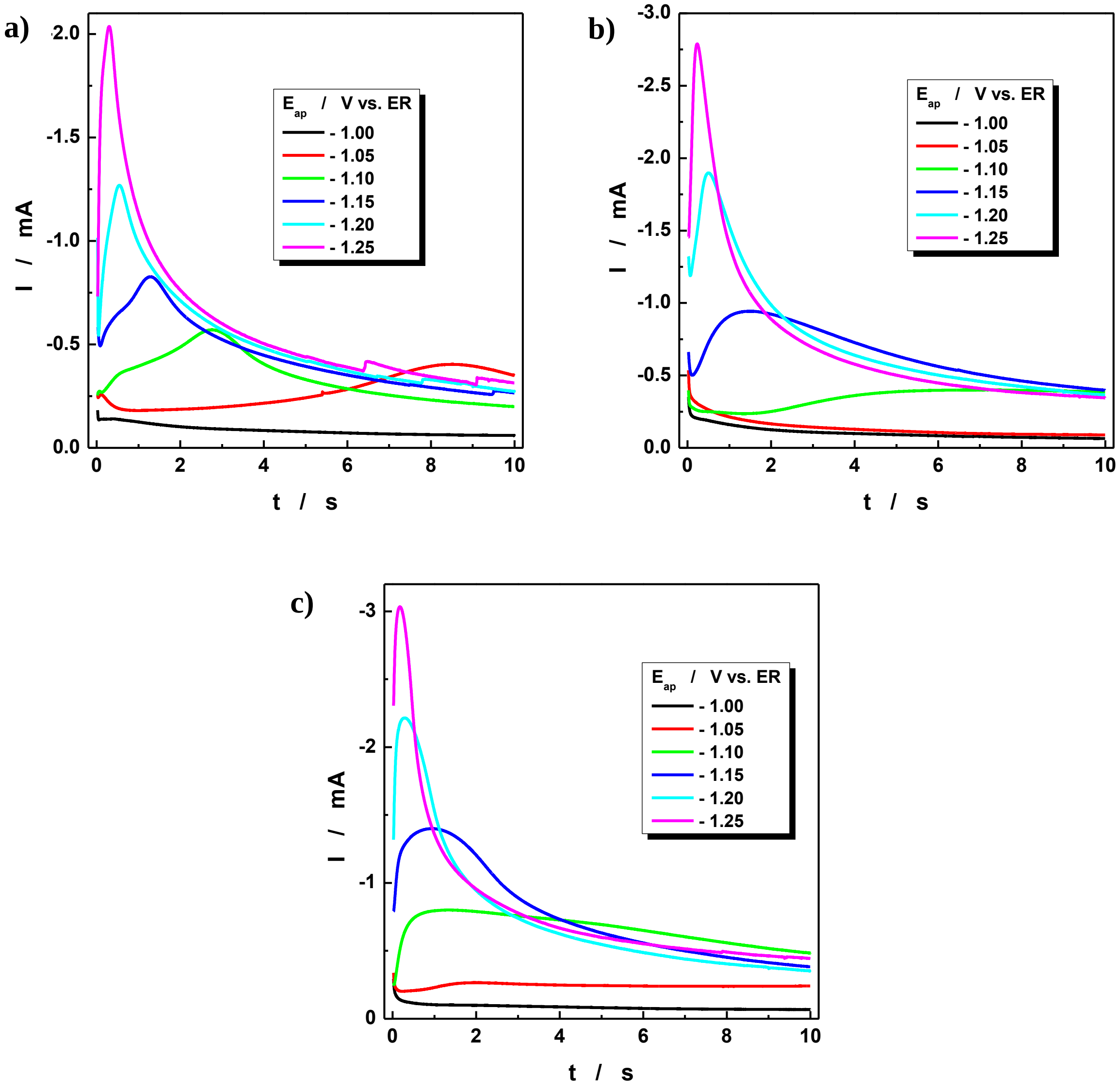

Figure 9 The chronoamperometric curves for Ni deposition (**a**), Fe deposition (**b**) and Ni-Fe co-deposition (**c**) for different applied potentials, pH = 3 [Robotin_2012a]

Using equations (1) and (2) and the graphical representation of $(I/I_m)^2$ *vs.* t/t_m, we obtained the theoretical curves for the two types of nucleation mechanisms [Scharifker_1983]. In our case, we calculated the ratio $(I/I_m)^2$ and plotted the values obtained for different values of the applied potential (see Figure 10). In order to determine the type of nucleation for the three cases mentioned above, the obtained curves were compared to the theoretical models.

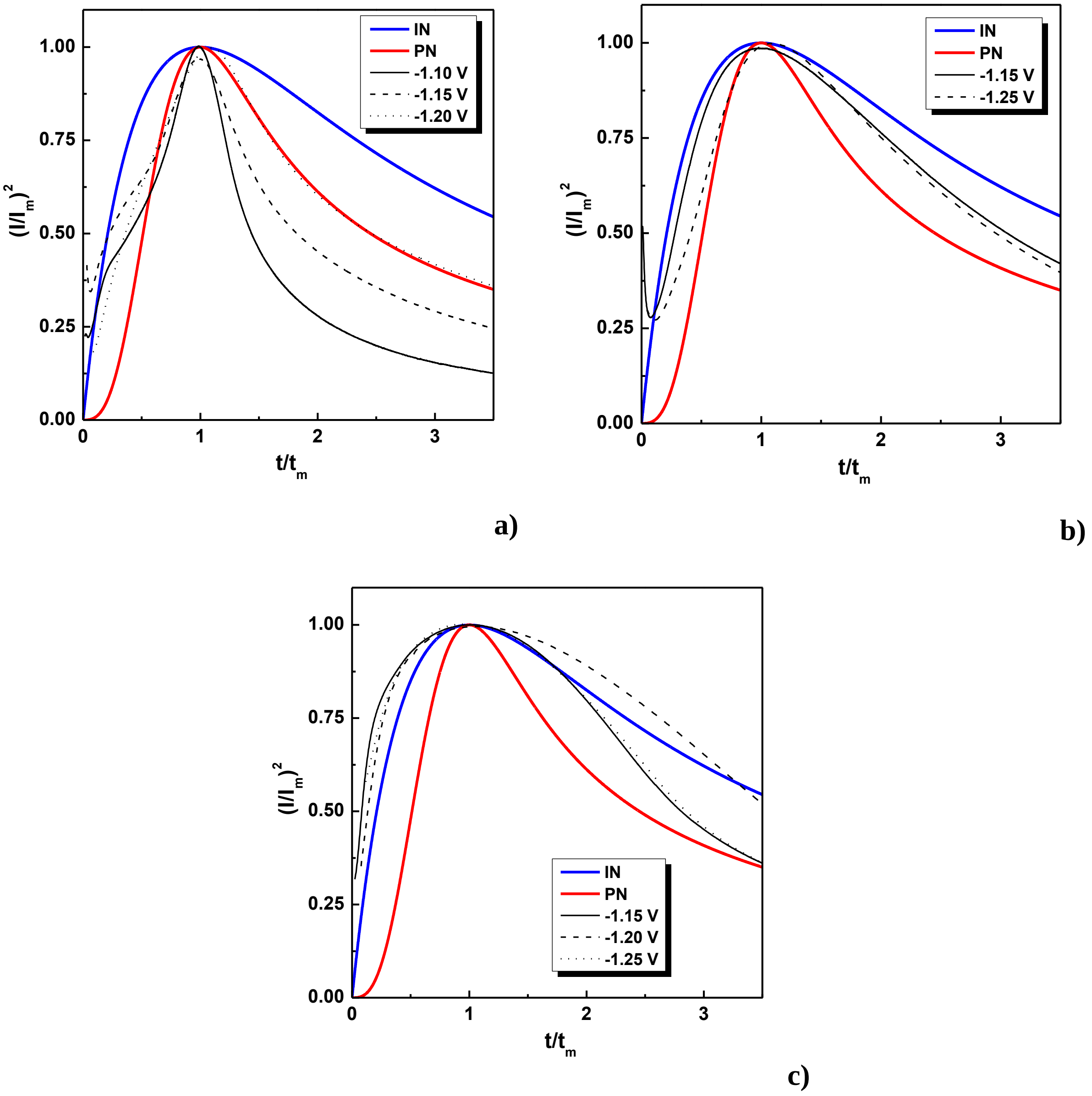

a)

b)

c)

Figure 10 Comparation between the theoretical curves for instantaneous and progressive nucleation and the experimental curves $(I/I_m)^2$ *vs.* t/t_m for the electrodeposition of **a)** Ni, **b)** Fe, and **c)** Ni-Fe from sulphate solutions, at different potentials (indicated in the figure legend) [Robotin_2012a].

As can be seen from Figure 10, the deposition of Ni is characterized by a progressive nucleation, while for Fe and Ni-Fe, the obtained experimental points are closer to the instantaneous nucleation model. The results are similar to those obtained by Su *et al.* in the case of Ni-Fe deposition from a fluoroborate solution [Su_2009]. The authors avoid assigning a clear mechanism for the electrodeposition of Ni-Fe since the potential curves show two distinct peaks for the Ni-Fe alloy. In the current study, the Ni-Fe alloy revealed a single larger peak, similar to the one obtained for the electrodeposition of Fe.

The differences between the nucleation mechanisms could explain the differences in the deposits' morphology for pure Ni and Ni-Fe alloys. The cracks appeared in the Ni-Fe deposits are due to the presence of Fe^{2+} ions which can influence the nucleation mechanism.

11. THE PROPOSED TECHNOLOGICAL FLOW DESCRIPTION

Based on the experimental results obtained in this thesis, a technological flow chart is proposed for the recovery of Ni from WEEE components, namely EG and SM, both components of CRTs. The stages of the technological flow chart shown in Figure 11 are described below [Robotin ISE_2012, Coman EFENSD_2012, Coman ICHMET_2012].

The first step consists in the manual processing of CRT waste, *i.e.* monitor **disassembly** and material **sorting** into components: **glass, ceramic, metal and plastic**. Next, the metal parts of EG and SM were dismantled and subjected to a magnetic separation process, thus obtaining two categories: one **magnetic fraction** (EGM) and another **non-magnetic fraction** (EGN). The SM is magnetic. This preliminary waste processing was done manually, but in can be done using to specific machines in order to implement it on an industrial scale.

In the next step, representative samples of EGM and EG were subjected to qualitative and quantitative analyses in order to establish their average compositions. Following the analysis, due to the high Ni content (75% of total Ni) of EGM components, these wastes are being processed for Ni recovery.

The next stage of the technological flow chart is represented by the **chemical and electrochemical leaching** of the EGM components. Due to unsatisfactory results obtained from chemical leaching (requires large amounts of concentrated mineral acids and long solubilisation times, the order of days), the electrochemical alternative proved to be the best solution. The leaching step generates solutions containing mainly Ni and Fe and low concentrations of Co and Mn. The further processing of these solutions can go two different ways:

i) **Ni-Fe alloys** or ternary Ni-Fe-Co alloys,

ii) **Metallic Ni** by electrowinning.

In order to obtain metallic Ni, Fe was removed from the solution in a number of steps. Firstly, Fe (II) was subjected to **electrochemical oxidation** in a two-compartment electrochemical reactor equipped with an anion exchange membrane. The next operation was the **separation of Fe (III)** by **precipitation**. **Metallic Ni** was electrowon from the resulting solutions after Fe removal.

Figure 11 The proposed technological flow for Ni recovery from CRT wastes [Robotin ISE_2012]

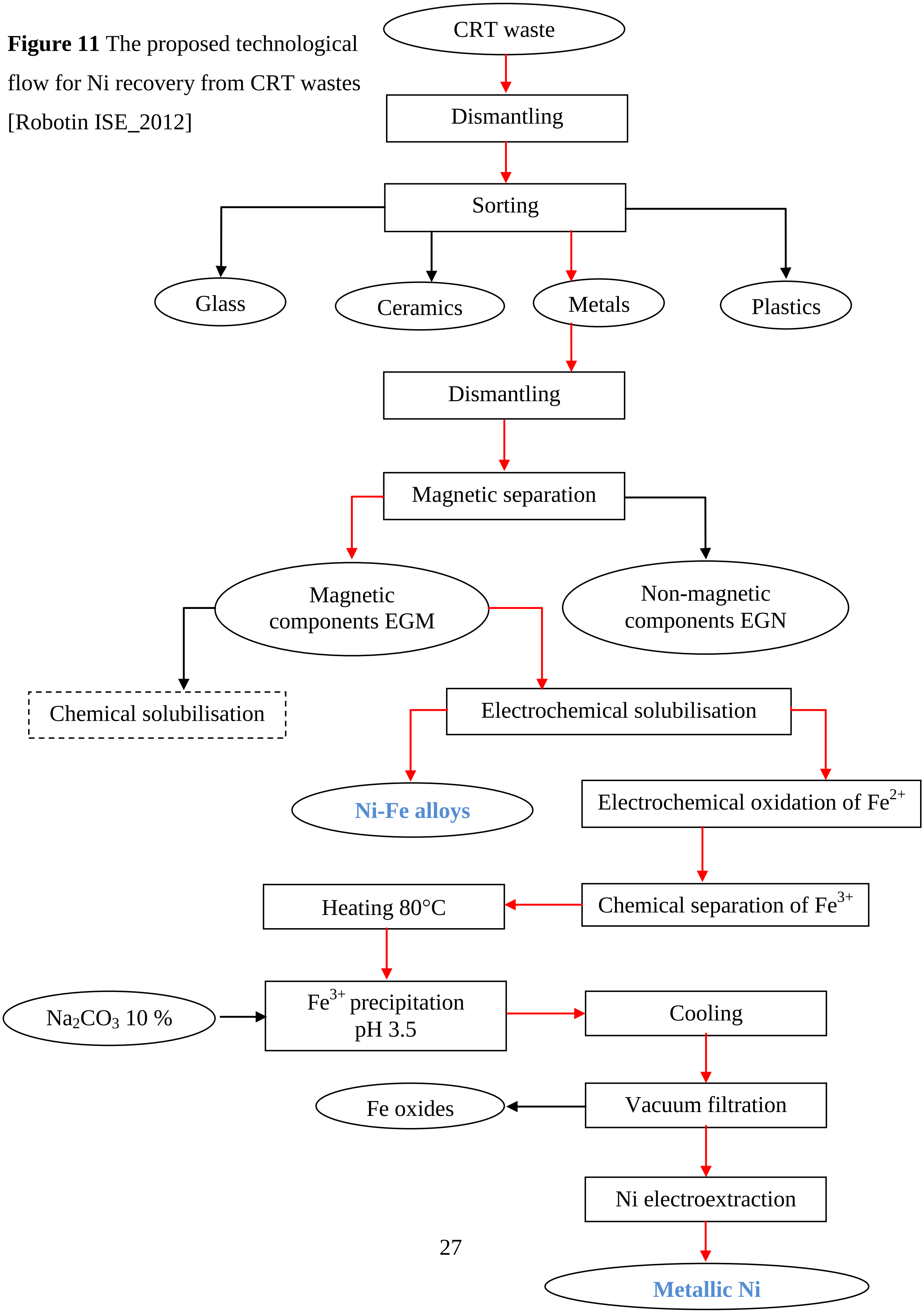

12. THE NICKEL RECOVERY FROM COMPUTER PRINTED CIRCUIT BOARDS (PCBs)

In this chapter we describe the recovery of nickel from other types of waste, particularly from computer motherboards. These wastes have a more complex composition than those studied in the earlier chapters; the metals contained in these waste include mainly the following: Cu, Fe, Ni, Sn, Pb, Zn.

The composition of the solution resulting after metal solubilization from 3 PCBs is given in Table 8.

Table 8 Metal composition (g/L) of the final solution, after metal solubilization from 3 PCBs and after excess Br_2 consumption

Metal →	**Cu**	**Fe**	**Ni**	**Pb**	**Sn**	**Zn**	**Total**
Concentration (g/L) →	6.29	9.36	0.33	0.89	0.33	12.57	29.77

In order to determine the values of the reduction potentials for the individual metals from the KBr medium, preliminary tests of voltammetry (cyclic and square wave) were carried out prior to any electrodeposition and cementation. A typical cyclic voltammogram is shown in Figure 12. A variety of overlapping reduction and oxidation peaks are visible, their separation couldn’t be possible even at lower scan rates scanning (10 mV s).

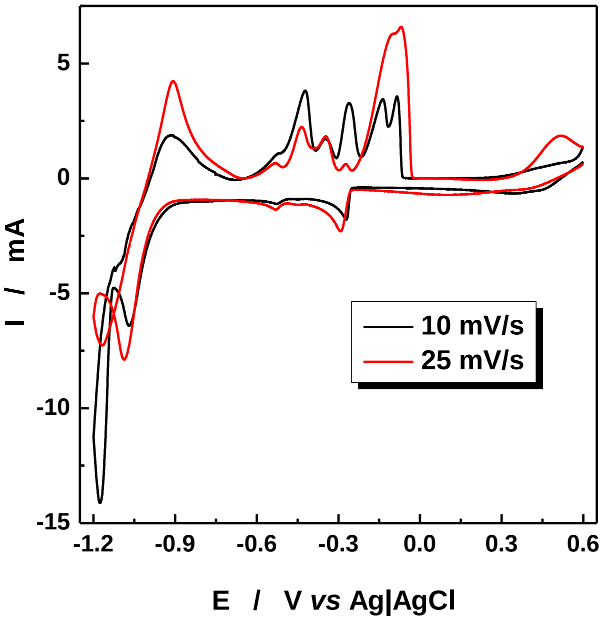

Figure 12 Cyclic voltammetry for the solution subjected to metal separation. The solution metallic composition is shown in Table 8

The cathodic electrodeposition tests for Cu, Sn and Pb were carried out in a two compartment reactor, the anode process being the oxidation of Br^- to Br_2. This process can be useful in the given circumstances, for the recirculation of the oxidizing agent used to remove the metals from PCBs. The electrodeposition experiments were carried out at constant potential in successive stages, each stage ending when the current value through the cell has reached relatively low values (below 10% of the initial value).

The first stage of the process was Cu electrodeposition at a potential value of -0.25 V, followed by steps where the applied potential values were decreased down to -0.7 V, resulting in the total electro-winning of Cu, Sn and Pb with no significant incorporation of Ni and Fe in the deposits. The composition of the deposits and electrolyte solutions was determined by FAAS after each step of electrodeposition. The analysis results are presented in Table **9**. In Table **9**, **S** stands for the electrolyte solution after each deposition step, **Si** being the initial solution and **Sf** the resulting solution after 4 electrodeposition steps. The deposits are denoted by **D**, and the numbers correspond to the following applied potential values: **01** to -0.25 V, **02** to -0.5 V, **03** to -0.6 V, and **04** to -0.7 V.

Table 9 The composition of the solution subjected to electrolysis and of the metal deposits after each potentiostatic electrodeposition step

Metal	**Cu**	**Fe**	**Ni**	**Pb**	**Sn**	**Zn**	**Total**
Si (g/L)	6.29	9.36	0.33	0.89	0.33	12.57	29.77
D01 (-0,25 V) (g)	1.621	BDL*	BDL *	BDL *	0.003	BDL *	1.624
S01 (g/L)	2.24	9.36	0.33	0.89	0.32	12.57	25.71
D02 (-0,5 V) (g)	0.538	BDL*	BDL *	0.043	0.105	BDL *	0.686
S02 (g/L)	0.89	9.36	0.33	0.78	0.06	12.57	23.99
D03 (-0,6 V) (g)	0.242	0.001	0.002	0.234	0.018	BDL *	0.498
S03 (g/L)	0.29	9.35	0.32	0.19	0.01	12.57	22.73
D04 (-0,7 V) (g)	0.115	0.001	0.003	0.075	0.003	BDL *	0.197
Sf (g/L)	BDL*	9.34	0.31	BDL *	BDL *	12.57	22.23

*below detection limit

As can be seen from Table **9**, 64.4% of the total Cu amount was electrowon from the solution, the deposit having 99.82 % purity in Cu. In this first stage a small amount of Sn was incorporated in the Cu deposit. In the second stage of electrodeposition (**D02**), at a value of the applied potential of -0.5 V, the resulted deposit incorporated Cu, Sn and Pb in the following proportions: 78.4% Cu, 15.3% Sn, and 6.3% Pb. In the third stage (**D03**), at a value of the applied potential of -0.6 V, the deposit contained 48.6% Cu, 47% Pb, 3.6% Sn, and a small amount of Ni and Fe (~ 0.6%). In our experience, the incorporation of small amounts of Ni and Fe at these potential values is promoted by the existing Cu ions in solution. In the last stage (**D04**), the deposit contains the rest of Cu, Sn, Pb remained in solution and small amounts of Ni and Fe. In this case the deposit composition is as follows: 58.4% Cu, 38.1% Pb, 1.5% Sn, 1.5% Ni and 0.5% Fe, respectively.

In the initial solution (**Si**) Ni represented 1.1% (mass) of the amount of dissolved metals, while in the resulting solution after electrodeposition of Cu, Sn and Pb (**Sf**), Ni represented 1.4% out of dissolved Ni, Fe and Zn. The next step aimed at concentrating Ni and the adopted method was its cementation using metallic Zn.

The resulted cement was separated from the solution by filtration, dissolved in aqua regia and analyzed by FAAS. Its relative composition (mass %) is given in Table 10.

Table 10 The composition (%) of the cement obtained by adding granules of zinc in a solution containing Ni, Fe and Zn

Cement →	**Ni**	**Fe**	**Zn**
Concentration (%) →	34	39	27

A technological flow diagram for the entire process is shown in Figure 13. The first step consisted in the **removing of radiators and condensers** with a significant content of Al. This prevents contamination of the solution and deposits with Al. The shredding and solubilization stage involves the fragmentation of the boards into small pieces that can be compacted in the chemical reactor, followed by the metal leaching in a setup consisting of a chemical reactor and a two-compartment electrochemical reactor. This stage resulted in obtaining a **metal deposit** and a **solution** containing dissolved metal ions. Cu was recovered from the electrolyte solution by **potentiostatic electrodeposition**. Traces of Cu, Sn and Pb were electrowon from the solution under potentiostatic deposition in **3 consecutive stages**. The resulting solution contained only Ni, Fe and Zn. In order to concentrate Ni, a **cementation stage** was employed using zinc granules. The result was a **metallic mixture of Ni, Fe and Zn**, out of which Ni represents a third of the total. The resulting solution after cement separation contains only Fe and Zn. **Fe can be separated** from the solution by precipitation (see Chapter 7). **Zn can be deposited** from the resulting solution as fibers and needles and reused in the cementing process. The final solution can be subjected to **an anodic oxidation process of Br^- to Br_2** in order to recirculate the oxidizing agent.

Figure 13 The proposed technological flow for Ni recovery from PCBs

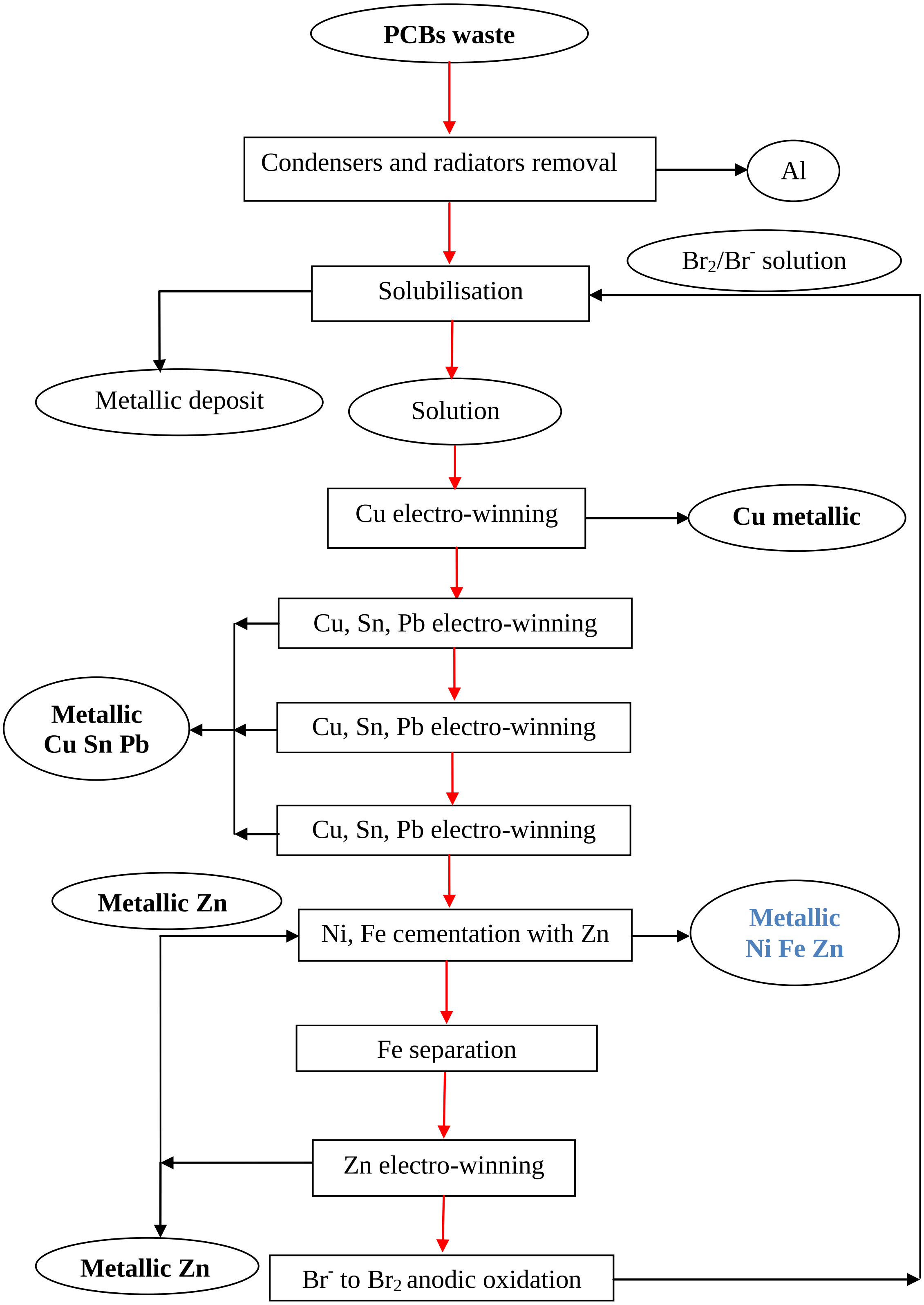

GENERAL CONCLUSIONS

In the first part of the thesis a literature overview on the Ni recovery from solid waste, wastewater and industrial secondary flows was made. Based on this overview the following conclusions can be stated:

- Given the complexity of waste composition, a specific approach is needed for each type of waste and the targeted characteristics of the final products.
- In order to recover nickel from solid waste a preliminary mechanical and chemical processing is necessary, followed by nickel leaching in solution and extraction by different techniques.
- Using different techniques - physical, chemical and electrochemical – in order to handle waste containing heavy metals is justified by the diversity of these wastes and the presence of several metals sometimes very difficult to separate (see Chapter 2, Section 2.4.).
- Ni recovery from different sources (secondary technological flows, used batteries, spent catalysts) was investigated.
- Depending on the concentration of nickel in solution different techniques may be employed. The advantages and disadvantages of the different techniques are given in Table 11.
- The most common Ni recovery techniques are ion exchange, solvent extraction and cathodic electrodeposition.
- The literature data provides information on the electrodeposition of Ni (see Chapter 3) from various aqueous solutions. These data refer to specific process parameters (current density, applied potential, composition of electrolyte solution, the influence of additives, pH and temperature). Thus a comparison with the data obtained in the present study is feasible.
- When using electrodeposition it is possible to obtain pure metal or its alloys.
- Since one of the objectives of the thesis is nickel recovery from waste in an alloy form, a bibliographic study was made for this purpose (see Chapter 4).
- For certain categories of waste electrical and electronic equipment (WEEE) there are no complete technologies for the treatment and recovery of nickel.

The second part of the thesis contains the results obtained for Ni recovery from waste cathode ray tubes and from computer motherboards. The conclusions are as follows:

- The electrochemical and structural investigative techniques for the studied systems have been described in detail (see Chapter 5).
- The importance of cathode ray tubes (waste used in this study for Ni recovery) recycling was emphasized, together with WEEE situation in Romania (see chapter 6, sections 6.1., 6.2., 6.3.).
- For an accurate description of the wastes to be studied, the results of their chemical analysis are given in Chapter 6, Section 6.5.
- Two types of leaching were studied, *i.e.* chemical leaching and electrochemical leaching. The electrochemical leaching proved to be more efficient than the chemical one. The best results in this case were obtained when working in a 2 M sulfuric acid medium (see Chapter 6, Section 6.6.).
- The research results have shown the necessity of Fe removal from solutions, given the high content of Fe in solutions resulted from CRT waste solubilization. This was possible through total oxidation of Fe(II) to Fe(III) and Fe(III) separation by precipitation.
- The oxidation of Fe (II) was performed electrochemically in a two compartment reactor equipped with an anion exchange membrane, the resulting process efficiency being 100% (see Chapter 7, Section 7.1.).
- Through precipitation it was possible to remove 99.9% of the total amount of Fe in solution, the nickel losses in precipitate being below 1%. Fe concentration in solution was reduced from 10 g/L to less than 10 mg/L. This step doesn’t have a negative influence on the Ni electrodeposition process, which follows the Fe separation step (see Chapter 7, Section 7.2.).
- The electrochemical study showed that it is possible to recover Ni by electrodeposition from solution resulting from EG dissolution if the total amount of Fe was removed from the solution.
- The current efficiencies for Ni electro-winning were around 95%. The specific energy consumption varied between 2.6 and 7.1 kWh/kg of deposited Ni (see Chapter 8, Section 8.3.).

- The current efficiency for Ni electrodeposition from binary (Ni - Co and Ni - Mn) and ternary (Ni – Co - Mn) solutions was between 37 and 92% (details in Chapter 8, Section 8.4.).
- EG recycling can result in the electrodeposition of Ni-Fe alloys from solutions resulting from the dissolution of these types of waste.
- Depending on the targeted applications for the Ni-Fe alloys (decorative, magnetic), a certain ratio of Ni-Fe can be obtained in the deposit by controlling the current density and the initial content of Fe in the electrolyte solution (see Chapter 9, Section 9.2.).
- The "normal" *vs.* "anomalous" behaviour were evaluated for the electrodeposition of Ni-Fe alloys (see Chapter 9, Section 9.2.3.).
- The difference in morphology for the Ni and Ni-Fe deposits suggests a difference in the nucleation mechanism for the two cases.
- In the case of Ni the electrodeposition process is achieved through a progressive nucleation mechanism, while for Fe and Ni-Fe, the results are closer to an instantaneous nucleation model (see Chapter 10, Section 10.2.).
- A technological flow was proposed for the recovery of nickel from waste cathode ray tubes (see Chapter 11).
- In the case of Ni recovery from PCBs, total removal of Cu, Sn and Pb from the solution was possible by running successive electrodeposition tests under controlled potentiostatic conditions, with no significant losses of Fe and Ni (see Chapter 12, Section 12.4.).
- Ni was recovered from solution by cementation with zinc in the form of a solid mixture of Ni, Fe and Zn, Ni concentration being approximately 33% of the mixture. In this way, we obtained a concentration of Ni in a ternary mixture, compared to the initial solution in which Ni represented 1.4% (0.31 g/L) of the total amount of metals (details in Chapter 12, Section 12.5.).
- A technological flow was proposed for the entire process, each of the 6 investigated metals (Cu, Sn, Pb, Ni, Fe, Zn) being recovered in a solid form.

REFERENCES

1. Abd El Aal, E. E.; Zakria, W.; Diab, A.; Abd El Haleem, S. M., Anodic dissolution of nickel in acidic chloride solutions. *Journal of Materials Engineering and Performance* **2003,** 12, (2), 172-178.

2. Agrawal, A.; Bagchi, D.; Kumari, S.; Kumar, V.; Pandey, B. D., Recovery of nickel powder from copper bleed electrolyte of an Indian copper smelter by electrolysis. *Powder Technology* **2007,** 177, (3), 133-139.

3. Andreola, F.; Barbieri, L.; Corradi, A.; Lancellotti, I., Cathode ray tube glass recycling: an example of clean technology. *Waste Management Research* **2005,** 23, 314-321.

4. Babu, B. R.; Parande, A. K.; Basha, C. A., Electrical and electronic waste: a global environmental problem. *Waste Management and Research* **2007,** 25, 307-318.

5. Bard, A. J.; Faulkner, L. R., *Electrochemical methods. Fundamentals and Applications*. Jonhn Willey & Sons, Inc.: New York, **2001**; Vol. II.

6. Bhattacharjee, S.; Gupta, K. K.; Chakravarty, S.; Thakur, P.; Bhattacharyya, G., Separation of Iron, Nickel, and Cobalt from Sulphated Leach Liquor of Low Nickel Lateritic Oxide Ore. *Separation Science and Technology* **2004,** 39, (2), 413-429.

7. Bigum, M.; Christensen, T. H., Waste electrical and electronic equipment. In *Solid waste technology and management*, Christensen, T. H., Ed. Blackwell Publishing: **2010**.

8. Borodi, G., Difractometru de raze X. In *Metode experimentale avansate pentru studiul și analiza bio-nano-sistemelor*, Aluaș, M.; Simon, S., Eds. Casa Cărții de Știință: Cluj-Napoca, **2012**.

9. Brenner, A., *Electrodeposition of alloys. Principle and Practice*. Academic Press: New York and London, **1963**; Vol. II.

10. Broekaert, J. A. C., *Analytical Atomic Spectrometry with Flames and Plasmas*. Willey-VCH: Wienheim, **2002**.

11. Chang, Y.; Zhai, X.; Li, B.; Fu, Y., Removal of iron from acidic leach liquor of lateritic nickel ore by goethite precipitate. *Hydrometallurgy* **2010,** 101, (1-2), 84-87.

12. Coman, V.; **Robotin, B**.; Dorneanu, S. A.; Ilea, P., Electrochemical studies on metal recovery from electronic waste. In *17th Romanian International Conference on Chemistry and Chemical Engineering* ***RICCCE*** *17*, Sinaia, România, **2011**.

13. Coman, V.; **Robotin, B**.; Ilea, P., Nickel recovery / removal from industrial wastes: A review. *Resources, Conservation and Recycling* **2012,** Under review.

14. Coman, V.; **Robotin, B**.; Ilea, P., Nickel recovery from electronic waste. In *Electrochemistry 2012, Fundamental and Engineering Needs for Sustainable Development, **EFENSD***, München, Germania, 2012.

15. Coman, V.; **Robotin, B.**; Ilea, P., Hydrometallurgical Processing and Recovery of Nickel from Spent Cathode Ray Tubes, *16th International Conference on Heavy Metals in the Environment, **ICHMET***, Roma, Italia, 2012.

16. Dousma, J.; De Bruyn, P. L., Hydrolysis-precipitation studies of iron solutions. I. Model for hydrolysis and precipitation from Fe(III) nitrate solutions. *Journal of Colloid and Interface Science* **1976,** 56, (3), 527-539.

17. Gangasing, D.; Talbot, J. B., Anomalous electrodeposition of nickel-iron. *Journal of the Electrochemical Society* **1991,** 138, (12), 3605-3611.

18. Havrilla, G. J., X-Ray Fluorescence Spectrometry. In *Handbook of instrumental techniques for analytical chemistry*, Settle, F., Ed. Prentice Hall PTR: 1997.

19. He, W.; Li, G.; Ma, X.; Wang, H.; Huang, J.; Xu, M.; Huang, C., WEEE recovery strategies and the WEEE treatment status in China. *Journal of Hazardous Materials* **2006,** 136, (3), 502-512.

20. Herat, S., Recycling of cathode ray tubes (CRTs) in electronic waste. *Clean* **2008,** 36, (1), 19-24.

21. Kaminari, N. M. S.; Schultz, D. R.; Ponte, M. J. J. S.; Ponte, H. A.; Marino, C. E. B.; Neto, A. C., Heavy metals recovery from industrial wastewater using Taguchi method. *Chemical Engineering Journal* **2007,** 126, (2-3), 139-146.

22. Lee, C. H.; Hsi, C. S., Recycling of scrap cathode ray tubes. *Environmental Science and Technology* **2002,** 36, 69-75.

23. Menad, N., Cathode ray tube recycling. *Resources, Conservation and Recycling* **1999,** 26, (3-4), 143-154.

24. Nnorom, I. C.; Osibanjo, O.; Ogwuegbu, M. O. C., Global disposal strategies for waste cathode ray tubes. *Resources, Conservation and Recycling* **2011,** 55, (3), 275-290.

25. Ongondo, F. O.; Williams, I. D.; Cherrett, T. J., How are WEEE doing? A global review of the management of electrical and electronic wastes. *Waste Management* **2011,** 31, (4), 714-730.

26. Pletcher, D., *A first course in electrode processes*. Alresford Press: Hants, **1991**.

27. Robinson, B. H., E-waste: An assessment of global production and environmental impacts. *Science of The Total Environment* **2009,** 408, (2), 183-191.

28. **Robotin, B**., Waste electrical and electronic equipment - a global concern. In *The International Conference Students for Students 9th Edition **SS***, Cluj-Napoca, România, **2012**.

29. **Robotin, B**.; Coman, V.; Ilea, P., Nickel recovery from electronic waste I. Nickel recovery from Cathode Ray Tubes. *Studia UBB Chemia* **2011,** LVI, (4), 121-130.

30. **Robotin, B**.; Coman, V.; Imre-Lucaci, F.; Ilea, P., Electrochemical studies of nickel recovery from cathodic ray tubes In *Journees d'Electrochimie **JE***, Grenoble, France, **2011**.

31. **Robotin, B.**; Imre-Lucaci, F.; Dorneanu, S. A.; Ilea, P., Recovery of nickel from waste electric and electronic equipments. In *The 14th International Conference of Physical Chemistry **Romphyschem** 14*, București, România, **2010**.

32. **Robotin, B**.; Ispas, A.; Coman, V.; Bund, A.; Ilea, P., Electrodeposition of Ni-Fe alloys from synthetic solutions similar to those obtained by electron gun recycling. In *Third Regional Symposium on Electrochemistry South-East Europe **RSE-SEE** 3*, București, România, **2012**.

33. **Robotin, B**.; Ispas, A.; Coman, V.; Bund, A.; Ilea, P., A Hydrometallurgical Process for Nickel Recovery from Cathode Ray Tube Waste. In *The 63rd Annual Meeting of the International Society of Electrochemistry **ISE***, Prague, Czech Republic, **2012**.

34. **Robotin, B**. **a.**; Ispas, A.; Coman, V.; Bund, A.; Ilea, P., Nickel recovery from electronic waste II Electrodeposition of Ni and Ni-Fe alloys from diluted sulfate solutions. *Waste Management* **2012,** Under review.

35. **Robotin, B**. **b.**; Coman, V.; Ilea, P., Nickel recovery from electronic waste: III Iron nickel separation. *Studia UBB Chemia* **2012,** Article accepted for publication.

36. Scharifker, B.; Hills, G., Theoretical and experimental studies of multiple nucleation. *Electrochimica Acta* **1983,** 28, (7), 879-889.

37. Sist, C.; Demopoulos, G., Nickel hydroxide precipitation from aqueous sulfate media. *JOM Journal of the Minerals, Metals and Materials Society* **2003,** 55, (8), 42-46.

38. Sneddon, J., Atomic absorption spectrometry. In *Handbook of instrumental techniques for analytical chemistry*, Settle, F., Ed. Prentice Hall PTR: 1997.

39. Su, C. w.; He, F. j.; Ju, H.; Zhang, Y. b.; Wang, E. l., Electrodeposition of Ni, Fe and Ni-Fe alloys on a 316 stainless steel surface in a fluorborate bath. *Electrochimica Acta* **2009,** 54, (26), 6257-6263.

40. Tudoran, L. B., Microscopul electronic de baleiaj și de transmisie. In *Metode experimentale avansate pentru studiul și analiza bio-nano-sistemelor*, Aluaș, M.; Simon, S., Eds. Casa Cărții de Știință: Cluj-Napoca, 2012.

41. Turdean, G. L., Metode electrochimice. In *Metode experimentale avensate pentru studiul și analiza bio-nano-sistemelor*, Aluaș, M.; Simon, S., Eds. Casa Cărții de Știință: Cluj-Napoca, 2012.

42. Vârvara, S. C.; Mureșan, L. M., *Metode electrochimice de investigare a electrodepunerii metalelor*. Casa Cărții de Știință: Cluj-Napoca, **2008**.

43. Wang, K.; Li, J.; McDonald, R. G.; Browner, R. E., The effect of iron precipitation upon nickel losses from synthetic atmospheric nickel laterite leach solutions: Statistical analysis and modelling. *Hydrometallurgy* **2011,** In Press, Corrected Proof.

44. Wang, K.; Li, J.; McDonald, R. G.; Browner, R. E., Nickel loss during iron precipitation and product characterization. In *Advanced Materials Research*, Beihai, 2012; Vol. 402, pp 293-296.

45. Wei, X.; Viadero Jr, R. C.; Buzby, K. M., Recovery of iron and aluminum from acid mine drainage by selective precipitation. *Environmental Engineering Science* **2005,** 22, (6), 745-755.

46. Widmer, R.; Oswald-Krapf, H.; Sinha-Khetriwal, D.; Schnellmann, M.; Böni, H., Global perspectives on e-waste. *Environmental Impact Assessment Review* **2005,** 25, (5), 436-458.

UNIUNEA EUROPEANĂ

GUVERNUL ROMÂNIEI
MINISTERUL MUNCII, FAMILIEI ŞI
PROTECŢIEI SOCIALE
AMPOSDRU

Fondul Social European
POSDRU 2007-2013

Instrumente Structurale
2007-2013

MINISTERUL
EDUCAŢIEI
CERCETĂRII
TINERETULUI
ŞI SPORTULUI

OIPOSDRU

UNIVERSITATEA BABEŞ-BOLYAI
CLUJ-NAPOCA

The authoress wish to thanks for financial support to the project:

Investing in people!

Ph.D. scholarship, Project co-financed by the SECTORAL OPERATIONAL PROGRAM FOR HUMAN RESOURCES DEVELOPMENT 2007 - 2013

Priority Axis 1. "Education and training in support for growth and development of a knowledge based society"

Key area of intervention 1.5: Doctoral and post-doctoral programs in support of research.

Contract nr.: **POSDRU/88/1.5/S/60185** – "INNOVATIVE DOCTORAL STUDIES IN A KNOWLEDGE BASED SOCIETY"

Babeş-Bolyai University, Cluj-Napoca, Romania

FONDUL SOCIAL EUROPEAN

Investeşte în
OAMENI

Titlul proiectului
„Studii doctorale inovative într-o societate bazată pe cunoaştere"
POSDRU/88/1.5/S/60185
Proiect cofinanţat din Fondul Social European
prin Programul Operaţional Sectorial Dezvoltarea Resurselor Umane
2007-2013

UNIVERSITATEA BABEŞ-BOLYAI
Departamentul Cercetare şi Management de Programe
Str. Universităţii, nr. 7-9, 400091 Cluj-Napoca
Tel. (00) 40 - 264 - 40.53.00*; int. 5329
Fax: 40 - 264 - 59.19.06
E-mail: bd.posdru2008@ubbcluj.ro